



Grant agreement no. 667510

GLINT

Research and Innovation Action
H2020-PHC-2015-two-stage

D4.7 Assessment of in vivo pH dependence of GlucoCEST contrast in mouse tumour models using CEST-based agents

Work Package:	4
Due date of deliverable:	30/06/2018
Actual submission date:	12/07/2018
Lead beneficiary:	UNITO
Contributors:	UNITO
Reviewers:	M. Rivlin (TAU)



Project co-funded by the European Commission within the H2020 Programme (2014-2020)		
Dissemination Level		
PU	Public	YES
CO	Confidential, only for members of the consortium (including the Commission Services)	
CI	Classified, as referred to in Commission Decision 2001/844/EC	

Disclaimer

The content of this deliverable does not reflect the official opinion of the European Union. Responsibility for the information and views expressed herein lies entirely with the author(s).

Contents

1	INTRODUCTION	4
2	METHODOLOGY AND APPROACH	5
2.1	Glucose preparation	5
2.2	Tumour models	5
2.2.1	Cell culture	5
2.2.2	Subcutaneous implantation	5
2.3	CEST MRI protocol.....	6
2.4	CEST analysis.....	6
3	ACTIVITIES CARRIED OUT AND RESULTS	8
4	CONCLUSIONS	12
5	BIBLIOGRAPHY / REFERENCES.....	13

1 Introduction

Previous in vitro results, described in the Deliverable 5.1, showed that glucose in a phosphate buffer solution provides higher GlucoCEST contrast at lower pH values and lower glucoCEST contrast at neutral pH values (at 37°C). Since tumours have low extracellular pH values as a consequence of elevated rates of glucose consumption combined with poor perfusion (hypoxia), such acidic environment can be encountered in the extracellular extravascular space of tumours when glucose or other glucose derivatives extravasate after intravenous administration.

The aim of this task is to assess the influence of the tumour extracellular pH on the measured MRI GlucoCEST contrast. In particular, the GlucoCEST signal will be evaluated in the same tumour model after sequential administration of glucose and of an established pH responsive agent (Iopamidol), allowing to simultaneously assess and correlate GlucoCEST MRI contrast with the extracellular tumour pH. Different tumour models (breast, melanoma and prostate cancer) will be investigated and two different metrics will be exploited to assess the pH dependence. Since the mouse will remain inside the MRI scanner following the double injection, besides a whole tumour comparison between average values, also a pixel-by-pixel comparison will be exploited for assessing such pH dependence.

2 Methodology and approach

2.1 Glucose preparation

Glucose solution for both intravenous and oral administration was prepared dissolving D-glucose (Sigma-Aldrich) in saline solution to obtain a 3 M solution (0.54 g/mL). The solution was then filtered with a 200 nm membrane filters in order to preserve the suspensions from bacterial contamination.

2.2 Tumour models

2.2.1 Cell culture

B16-F10 (mouse melanoma cells), 4T1 (mouse mammary carcinoma) and PC3 (human prostate cancer) cells were obtained from American Type Culture Collection (ATCC). B16-F10 cells were cultured in EMEM supplemented with 10% FBS, 100 µg/ml penicillin and 100 µg/ml streptomycin; 4T1 cells were grown in RPMI 1640 medium supplemented with 10% FBS, 100U/mL (Pen/Strep) and 2 mM L-Glutamine; PC3 cells were cultured in Ham's F-12 supplemented with 10% FBS, 100 µg/ml penicillin and 100 µg/ml streptomycin. The cells were grown at 37°C in a humidified atmosphere containing 5% CO₂.

2.2.2 Subcutaneous implantation

Male C57BL/6 mice (Charles River Laboratories Italia S.r.l., Calco Italia), female BALB/c mice (Envigo RMS, S.r.l., Udine Italia) and male Athymic Nude-Foxn1nu mice (Envigo RMS, S.r.l., Udine Italia) were maintained under specific pathogen free conditions in the animal facility of the Center for Preclinical Imaging, University of Turin, and treated in accordance with the University Ethical Committee and European guidelines under directive 2010/63. Male C57BL/6 mice were inoculated with 5.0 x 10⁵ B16-F10 melanoma cells in both flanks 10 days before imaging acquisition; female BALB/c mice were inoculated with 4.0 x 10⁴ 4T1 cells in both flanks 15 days before imaging acquisitions; male Athymic Nude-Foxn1nu mice were inoculated with 5 x 10⁶ cells in both flanks 30 days before imaging acquisitions.

Before imaging, mice were anesthetized by isoflurane, placed on the MRI bed and an air pillow placed below the animal (SA Instruments, Stony Brook, NY; USA) monitored breath rate. The tail vein was cannulated with a catheter to administer glucose (doses of 3 g/kg and of 5 g/kg)

or iopamidol through a 27-gauge needle; mice received the same dose of iodinated contrast media of 4 g iodine/kg body weight, slowly injected via the same catheter without removing the animal from the MRI scanner.

2.3 CEST MRI protocol

MR images were acquired with a Bruker 7T Pharmascan scanner (Bruker Biospin, Ettlingen, Germany) equipped with a 30mm 1H coil.

After the scout image acquisition, T2w anatomical images were acquired with a RARE sequence and the same geometry was used for the following CEST experiments.

The GlucoCEST images were obtained by RF irradiation with a single continuous wave presaturation block pulse of $2\mu\text{T}$ applied for 5 sec. The saturation frequency offset was varied between 6 and -6 ppm with a frequency resolution of 0.2 ppm. MR images were acquired using a Spin Echo RARE sequence (TR/TE/NEX/Rare Factor 6.0 sec/4.7 msec/1/64); centric encoding, field of view = 3 cm x 3 cm; slice thickness = 2 mm; matrix = 64 x 64.

Each mouse was administered with a bolus injection of ca. 0.12 mL glucose solution at dose 5g/kg (n=8 for each tumour model). (A first study was conducted administrating a dose of glucose at 3g/Kg, but since not enough contrast was detectable in the whole tumour regions, a higher dose was administered. Here are presented only the results obtained from the 5g/Kg glucose dose administration).

Z-spectra before and after iodinated contrast media injection were acquired in the frequencyoffset range ± 10 ppm using a single-shot RARE sequence with centric encoding (TR/TE/NEX/Rare Factor = 6.0 s/4.7 msec/1/64) preceded by a $3\mu\text{T}$ cw block presaturation pulse for 5 s. We used an acquisition matrix of 64×64 for a field of view of 3×3 cm (in-plane spatial resolution = 312.5 μm) with a slice thickness of 2 mm. Between the two injection, a 30 minutes of washout time was considered.

2.4 CEST analysis

All the CEST images were elaborated in MATLAB (The Mathworks, Inc., Natick, MA, USA) using custom scripts. Anatomical and Z-spectrum images were first segmented by using an intensity-threshold filter (1). The Z-spectra were interpolated, on a voxel-by-voxel basis, by

smoothing splines (2) to identify the correct position of the bulk water, thus removing artefacts arising from B0 inhomogeneity. On this basis, the interpolated Z-spectrum was shifted so that the bulk water resonance corresponds to the zero frequency and corrected intravoxel saturation transfer (ST) effects were calculated. Then, a second filter was applied to remove CEST effect arising from noisy data, calculating the coefficient of determination R2 for the interpolating curve to take into account the signal-to-noise ratio of single voxels (noisy Z-spectra present low R2 values). Only voxels with high R2 (>0.99) were considered in the ST% calculation.

The ST effect for glucose (GlucoCEST) was estimated from the expression:

$$ST = \frac{S(-1.2ppm) - S(1.2ppm)}{S_0} \quad [1]$$

where S_0 was the signal at -10ppm.

The ST effect for iopamidol (iopamidol CEST) was estimated from the expression:

$$ST = \frac{S(-4.2ppm) - S(4.2ppm)}{S_0} \quad [2]$$

where S_0 was the signal at -10ppm.

Results are reported as:

$$\Delta ST \% = [(ST \text{ post injection} - ST \text{ pre injection}) * 100]$$

The correlation between the GlucoCEST contrast and the tumour extracellular pH was measured by calculating the average values of GlucoCEST contrast and pH for each tumour.

Moreover, to better investigate the spatial correlation between glucoCEST and tumour pH, a similarity analysis was performed pixel-by-pixel. For each tumour only pixels where both glucose and Iopamidol were detectable ($\Delta ST > 2\%$) were considered. The correlation coefficients between glucoCEST and iopamidol CEST, as well as between GlucoCEST and tumour pH was calculated for all these pixels.

3 Activities carried out and results

In order to determine *in vivo* the influence of the tumour extracellular pH on the GlucoCEST contrast, CEST images of three different tumour model (B16-f10, 4T1 and PC3) were acquired on a 7T scanner. Each mouse underwent sequential intravenous injections of glucose (5g/Kg) and after 30 minutes, to allow the washout of glucose molecule from the tumour region, of iopamidol (4 g I/Kg).

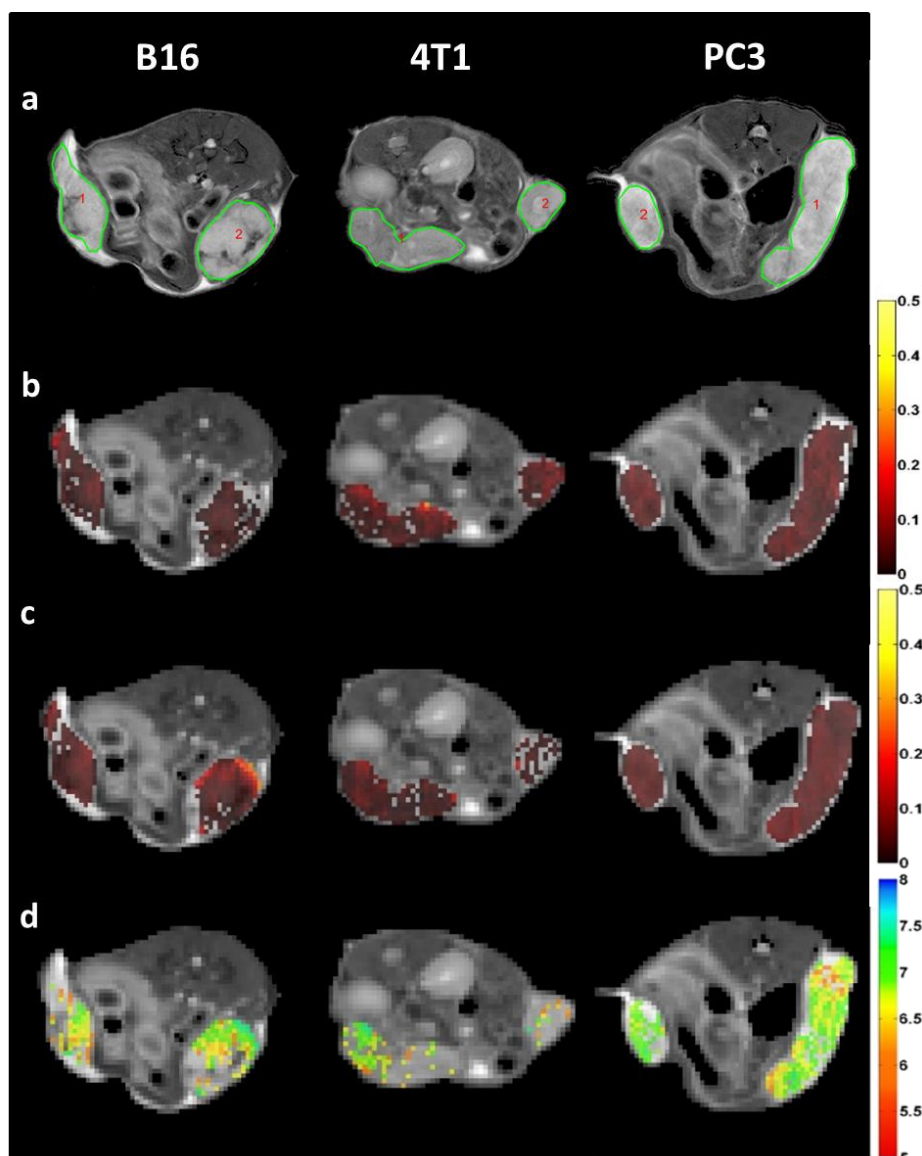


Figure 1: **a**, Anatomical T₂ weighted images of representative B16, 4T1 and PC3 tumour bearing mice. **b**, Representative GlucoCEST map overimposed on the anatomical image of each tumour model obtained after i.v. injection of D-glucose, 5 g/kg (Data are reported as the difference, Δ ST %, between the ST effect before and after the intravenous injection). **c**, Representative contrast enhanced maps upon i.v. injection of iopamidol as MRI-CEST Δ ST% maps of each tumour model (Data are reported as the difference, Δ ST %, between the ST effect

before and after the intravenous injection). **d**, Tumour pH map overlaid on the anatomical image of each tumour model obtained upon iopamidol injection.

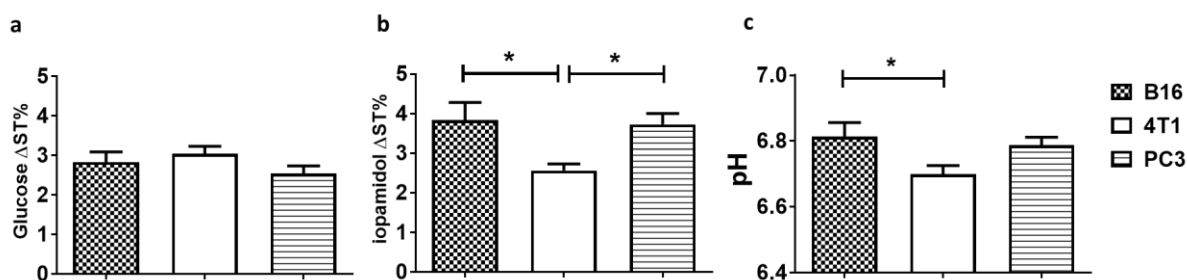


Figure 2: **a**, Mean GlucoCEST contrast obtained injecting glucose solution at 5g/Kg dose via intravenous bolus for each tumour model. Data are reported as the variation (Δ ST%) between the ST effect percentage post minus pre intravenous injection. **b**, Mean iopamidol contrast enhancement (Δ ST%) for each tumour model. **c**, Mean pH value calculated for each tumour model.

As shown from representative CEST contrast map and in Figure 2b, the three different tumour models displayed a similar glucoCEST contrast (glucose Δ ST%= 2.83, 3.04 and 2.54 for B16-f10, 4T1 and PC3, respectively). B16-f10 and PC3 tumour showed higher iopamidol CEST contrast than 4T1 tumours (iopamidol Δ ST%: 3.83, 2.56 and 3.73 for B16, 4T1 and PC3, respectively). Moreover, the 4T1 tumour model presented a more acidic pH than B16-f10 and PC3 models (mean tumour pH value = 6.81, 6.69 and 6.78 for B16, 4T1 and PC3, respectively).

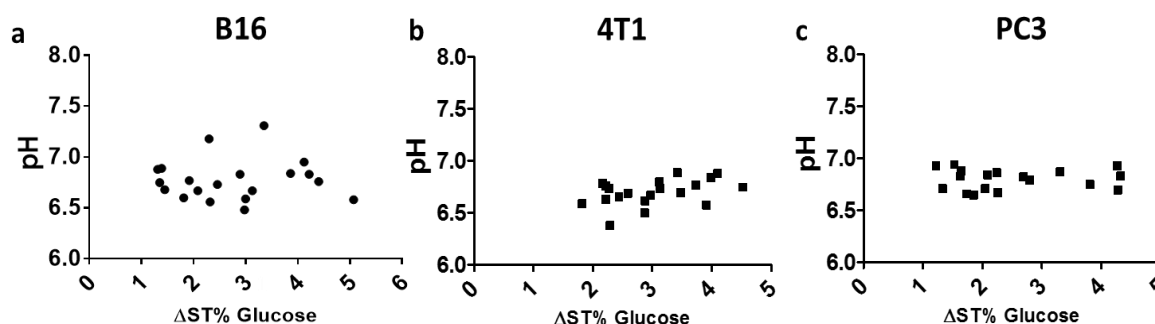


Figure 3: **a**, correlation scatterplot of mean pH value and mean Δ ST% Glucose contrast for B16, 4T1 (**b**) and PC3 (**c**) tumour model.

GlucoCEST contrast and tumor pH values were correlated by calculating the average values for each metric in the whole tumor region. In vivo we did not observe a clear pH dependence with the GlucoCEST contrast in the tumor regions. As shown in Figure 3, a wide range of GlucoCEST contrast (Δ ST% 1-5%) was observed in a physiological range of tumor extracellular pH values (pH: 6.4-7.1) for each tumor model. Exploiting the sequential

administration of the two CEST agents, we performed a correlation of the two metrics inside the tumor using a pixel-by-pixel approach.

First, we identified pixels within the same tumour region where both glucose and iopamidol were detectable (Figure 4, pixels coloured in blue). For these pixels, we correlated the GlucoCEST contrast and the measured tumour pH values within the same tumours. Figure 4 shows representative similarity maps of B16-f10, 4T1 and PC3 tumour model and scatterplot correlation graph between GlucoCEST contrast iopamidol CEST and between GlucoCEST and tumour pH for each tumour.

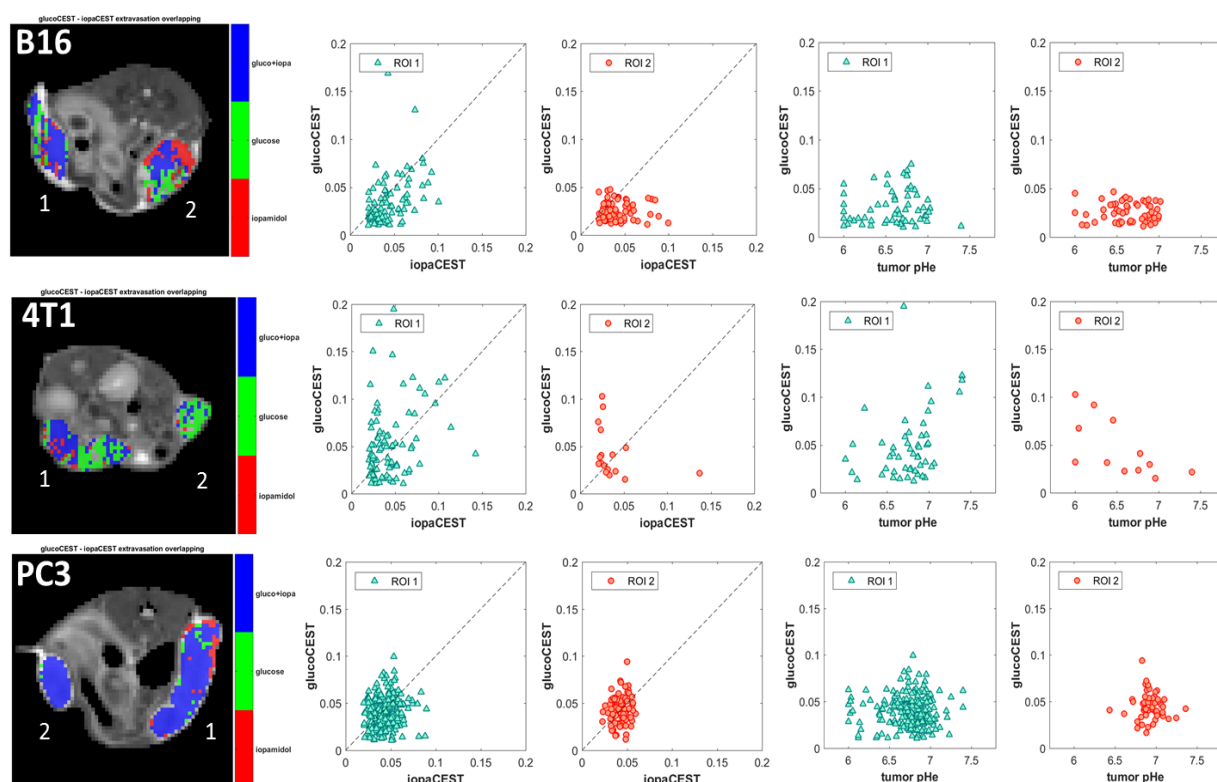


Figure 4: Representative similarity maps overlaid on the anatomical images for each tumour model showing pixels where both glucose and iopamidol have been detected (blue pixels) or when only one CEST agent has been detected (red and green, for iopamidol or glucose, respectively). Scatterplot correlation graphs of each representative tumour ROI between glucoCEST contrast and iopamidol CEST contrast or between glucoCEST contrast and tumour pH values calculated for pixel by pixel.

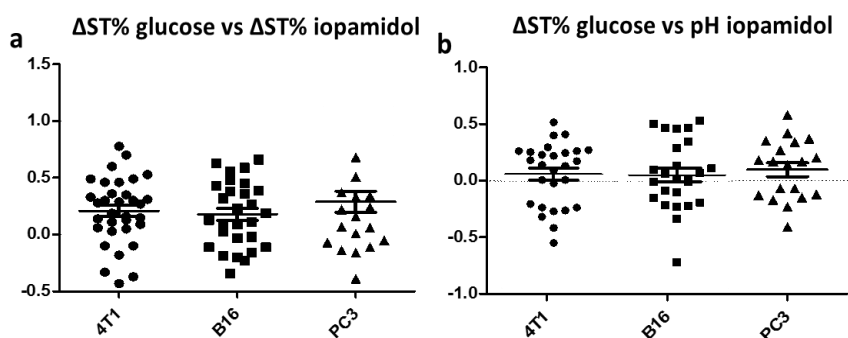


Figure 5: **a**, Similarity analysis between GlucoCEST (Δ ST% Glucose) and Iopamidol CEST (Δ ST% iopamidol) calculated pixel by pixel. **b**, Spatial similarity between GlucoCEST contrast (Δ ST% Glucose) and pH value for each tumour.

We observed a moderate spatial correlation between pixel-by-pixel glucoCEST and Iopamidol CEST contrast, with a wide range of correlations both positive and negative, for different tumours even within the same murine tumour model. Also, the correlation between GlucoCEST and tumour pH showed a big variability, with some tumours showing high correlation between GlucoCEST contrast and the acidic tumour microenvironment and others showing moderate or no relationship.

4 Conclusions

The aim of this task was to assess in vivo the pH dependence of the glucoCEST contrast. High glucose dose was injected (5g/Kg) to ensure good contrast revelation at 7T field and three different tumour model were investigated. Based on the previous in vitro studies, one would expect that a more acidic tumour would display a higher GlucoCEST contrast in comparison to less acidic tumours. A wide variability in the amount of GlucoCEST contrast was observed in the three investigated murine tumour models that was reflected by a large difference in mean tumour pH values, despite all the three tumour models showed acidic tumour microenvironment.

A large heterogeneity in tumour pH was observed, resulting in pH dependence of the GlucoCEST contrast only in some tumours or in some tumour regions. Several factors may influence the observed GlucoCEST contrast, besides the extracellular tumour pH, since also vascularization and permeability may affect the distribution and the accumulation of the injected tracer within the extracellular space, as well as the different distribution of the two tracers in the extracellular or in the intracellular compartments. Moreover, since mice have not been fasted the night before the injection of glucose, this may result in a lower glucoCEST contrast, albeit enough contrast (ca. 3%) was observed within the tumour region to be correlated with the extracellular pH measurement.

5 Bibliography / References

1. Chu V, Hamarneh G. MATLAB–ITK interface for medical image filtering, segmentation, and registration. Proc SPIE Med Imaging: Image Process 2006;6144:1–8.
2. Stancanello J, Terreno E, Castelli DD, Cabella C, Uggeri F, Aime S. Development and validation of a smoothing-splines-based correction method for improving the analysis of CEST-MR images. Contrast Media Mol Imaging 2008;3:136–149.